Research article JHEP|Reports

Biliary tract cancer patient-derived xenografts: Surgeon impact on individualized medicine

Authors

Jennifer L. Leiting, Stephen J. Murphy, John R. Bergquist, Matthew C. Hernandez, Tommy Ivanics, Amro M. Abdelrahman, Lin Yang, Isaac Lynch, James B. Smadbeck, Sean P. Cleary, David M. Nagorney, Michael S. Torbenson, Rondell P. Graham, Lewis R. Roberts, Gregory J. Gores, Rory L. Smoot, Mark J. Truty

Correspondence

Truty.Mark@mayo.edu (M.J. Truty).

Graphical abstract

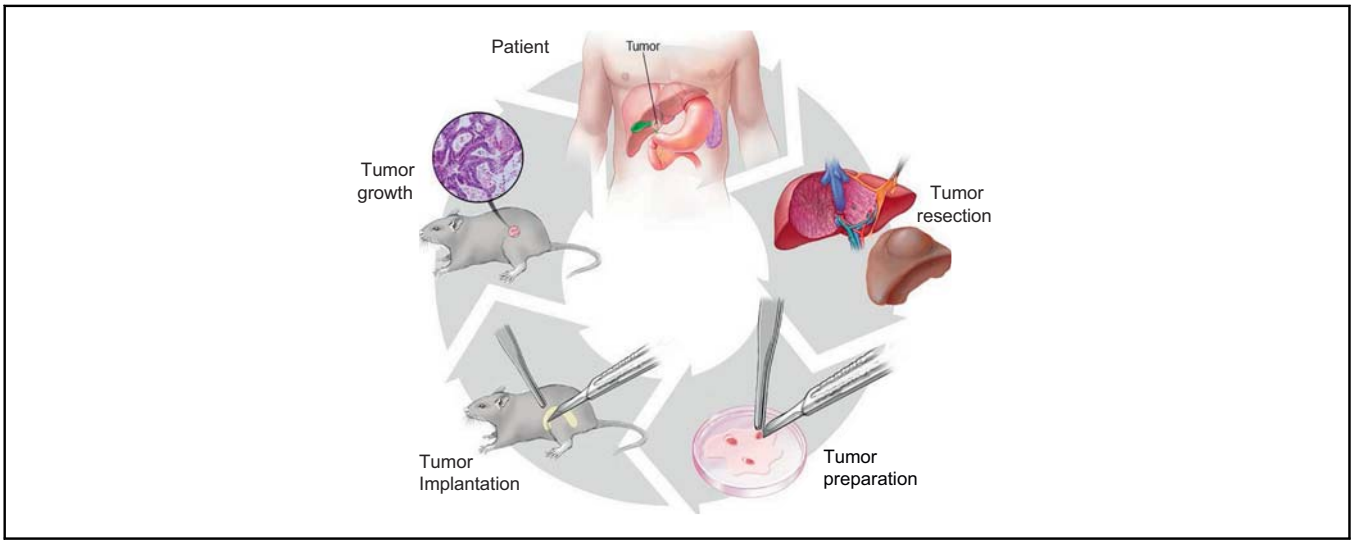

Highlights

- Biliary tract tumors are uncommon but highly aggressive malignancies with poor survival outcomes.
- Patient-derived xenografts preserve the unique histology and genetic characteristics of the original patient tumor.
- Successful engraftment is an independent predictor for worse recurrence-free patient survival.
- Patients with tumors containing tetraploid genomes had worse overall survival.

Lay summary

Patient biliary tract tumors grown in immunocompromised mice are an invaluable resource in the treatment of biliary tract cancers. They can be used to guide individualized cancer treatment in high-risk patients.

https://doi.org/10.1016/j.jhepr.2020.100068

Research article

JHEP|Reports

Biliary tract cancer patient-derived xenografts: Surgeon impact on individualized medicine

Jennifer L. Leiting,[1] Stephen J. Murphy,[2] John R. Bergquist,[1] Matthew C. Hernandez,[1] Tommy Ivanics,[3] Amro M. Abdelrahman,[1] Lin Yang,[2] Isaac Lynch,[1] James B. Smadbeck,[2] Sean P. Cleary,[1] David M. Nagorney,[1] Michael S. Torbenson,[4] Rondell P. Graham,[4] Lewis R. Roberts,[5] Gregory J. Gores,[5] Rory L. Smoot,[1] Mark J. Truty[1,*]

[1]*Department of Surgery, Mayo Clinic, Rochester, MN;* [2]*Center for Individualized Medicine, Mayo Clinic, Rochester, MN;* [3]*Department of Surgery, Henry Ford Medical Center, Detroit, MI;* [4]*Department of Pathology, Mayo Clinic, Rochester, MN;* [5]*Department of Gastroenterology and Hepatology, Mayo Clinic, Rochester, MN*

JHEP Reports **2020.** https://doi.org/10.1016/j.jhepr.2020.100068

Background & Aims: Biliary tract tumors are uncommon but highly aggressive malignancies with poor survival outcomes. Due to their low incidence, research into effective therapeutics has been limited. Novel research platforms for pre-clinical studies are desperately needed. We sought to develop a patient-derived biliary tract cancer xenograft catalog.
Methods: With appropriate consent and approval, surplus malignant tissues were obtained from surgical resection or radiographic biopsy and implanted into immunocompromised mice. Mice were monitored for xenograft growth. Established xenografts were verified by a hepatobiliary pathologist. Xenograft characteristics were correlated with original patient/tumor characteristics and oncologic outcomes. A subset of xenografts were then genomically characterized using Mate Pair sequencing (MPseq).
Results: Between October 2013 and January 2018, 87 patients with histologically confirmed biliary tract carcinomas were enrolled. Of the 87 patients, 47 validated PDX models were successfully generated. The majority of the PDX models were created from surgical resection specimens (n = 44, 94%), which were more likely to successfully engraft when compared to radiologic biopsies ($p = 0.03$). Histologic recapitulation of original patient tumor morphology was observed in all xenografts. Successful engraftment was an independent predictor for worse recurrence-free survival. MPseq showed genetically diverse tumors with frequent alterations of *CDKN2A, SMAD4, NRG1, TP53*. Sequencing also identified worse survival in patients with tumors containing tetraploid genomes.
Conclusions: This is the largest series of biliary tract cancer xenografts reported to date. Histologic and genomic analysis of patient-derived xenografts demonstrates accurate recapitulation of original tumor morphology with direct correlations to patient outcomes. Successful development of biliary cancer tumografts is feasible and may be used to direct subsequent therapy in high recurrence risk patients.

Introduction

Biliary tract cancers, including cholangiocarcinoma and gallbladder carcinoma, are a diverse group of epithelial tumors that are among the most lethal of malignancies.[1] In the majority of cases, patients present with incurable locally advanced or metastatic disease with an overall 5-year survival of only 5–10%.[2,3] A small fraction of patients will present with disease amenable to surgical resection, however, these operations are associated with significant morbidity and mortality risk.[4,5] Furthermore, those patients able to undergo curative intent resection can expect a high rate of post-resection recurrence with limited subsequent overall survival.[6,7] Chemotherapy options are limited as traditional cytotoxic agents have shown only modest overall efficacy and targeted approaches have yet to be proven effective.[8–10]

The use of established cell lines and cell line-derived xenograft models has been the mainstay of basic and translational research into the mechanisms of disease for biliary cancers because they are convenient, reliable, and reproducible.[11] However, their translational value is of limited clinical value.[12] It is known that *in vitro* models are subject to significant pheno- and genotypic deviation from their tumor of origin.[13,14] The interactions between tumor cells and surrounding stromal components including extracellular matrix (ECM) are known to influence key cell cycle triggers of proliferation, migration, and apoptosis and these interactions are not recapitulated in such models.[15,16] Additionally, cell line and *in vitro* models have limited ability to recapitulate cell-cell signaling and tumor microenvironment effects including the influence of hypoxia on tumor growth, which further alter gene expression and behavior

Keywords: Patient-derived xenografts; biliary tract; cholangiocarcinoma; gallbladder carcinoma; MatePair sequencing.
Received 24 August 2019; received in revised form 8 January 2020; accepted 8 January 2020; available online 16 January 2020
* Corresponding author. Address: Division of Hepatobiliary and Pancreas Surgery, Mayo Clinic, 200 First St. Southwest, Rochester, MN 55902. Tel.: +001 (507) 284 2166, fax: +001 (507) 284-5196.
E-mail address: Truty.Mark@mayo.edu (M.J. Truty).

of tumor cells.[17,18] Cell lines in particular have been found to have more resemblance to cell lines derived from other tumor types than to the original clinical sample they were derived from, and previous work has shown little to no correlation with clinical therapeutic efficacy.[19] These limitations restrict the translational value of studies performed with traditional cell line models.

Patient-derived xenografts (PDX) are preclinical models that preserve the specific and unique histology and genetic characteristics of the original patient tumor.[20] They possess the biological heterogeneity and individual patient phenotype that is not present in other preclinical models and can be used to assess response to treatment regimens with high correlation and positive predictive value.[21] PDX models can also be used to predict a patient's clinical course and likelihood for recurrence.[22] While there have been descriptions of the establishment of a limited number of biliary tract cancer PDX models, here we describe the largest biliary tract PDX library reported to date.[23–27]

Methods

Patient cohort

With Institutional Review Board and Institutional Animal Care and Use Committee approval, patients presenting for resection or biopsy of biliary tract cancers were informed regarding the research study. Consent was obtained and patient information was acquired by review of the electronic medical record. After xenograft implantation, patient information including tumor type, location, date of recurrence, adjunctive therapies, and mortality were obtained periodically.

Acquisition of tissue

A pictoral representation of the tissue acquisition and implantation process can be found in Fig. 1A. After initial rapid clinical pathologic review of the resected tissue was complete and the presence of surplus tumor tissue was verified, study personnel obtained surplus tumor tissue and immediately placed it in ice-cold Roswell Park Memorial Institute 1640 medium (Invitrogen, Carlsbad, CA) with 10% FBS (Atlanta Biologicals, Flowery Branch, GA) and 1% antibiotic-antimycotic 100× (ThermoFisher, Waltham, MA). Tissue ischemic time was computed as the time of specimen removal from the patient until the time of tissue implantation into the mouse.

Implantation procedure

Upon arrival in the lab, tissue was removed from its medium and cut into 1 mm^3 pieces in a sterile petri dish maintained on ice. Matrigel (Corning, Corning, NY) was added to the dissected tissue pieces. Concurrently, 5 NOD/SCID mice (Department of Comparative Medicine, Rochester, MN) were placed under general anesthesia. Following sterile preparation with 70% ethanol, one of the previously prepared pieces of tumor specimen was implanted in the right flank and the same procedure was followed on the left side for bilateral implantation. After procedure completion, mice were returned to their storage boxes and observed for complications.

Observation for xenograft growth

Tumor formation was monitored by direct palpation and growth was recorded using digital calipers in a weekly-maintained database using RedCap software.[28] The date of first tumor formation was recorded when a mass of approximately 8 mm^3 was palpable. The date of first tumor harvest was recorded when the

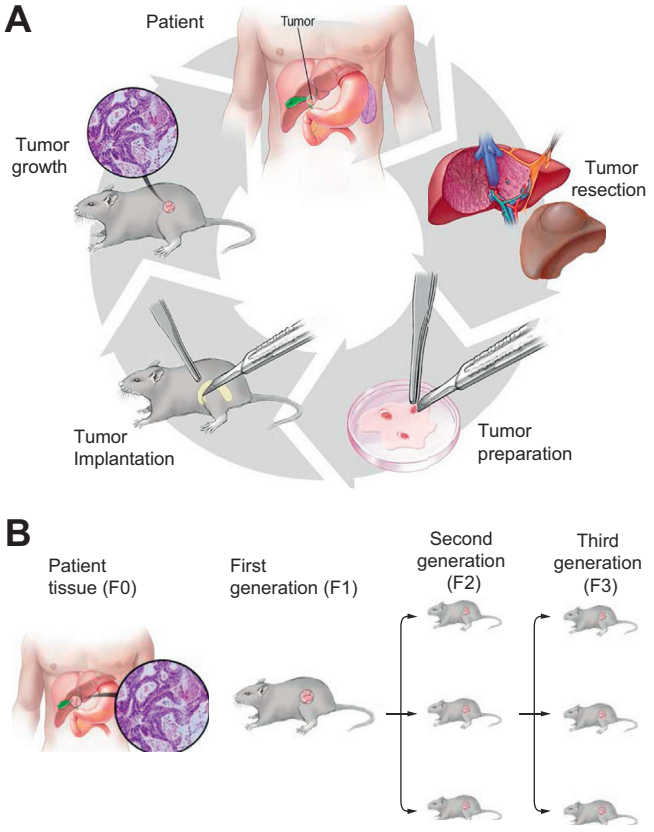

Fig. 1. Patient-derived xenograft implantation and passage. The process for implantation and engraftment of patient-derived xenograft models (A) and the passage of verified tissue into subsequent generations (B).

tumors had reached a volume of 1,000 mm^3. Time to tumor formation (TTF) was calculated from the date of implantation to the date of first tumor formation (days). Time to tumor harvest (TTH) was calculated from the date of implantation to the date of first tumor harvest (days) based on institutional policies on maximal tumor size. Engraftment efficiency was calculated as the number of mice per individual patient tumor that grew successful xenografts/total number of mice implanted for that patient tumor. Overall patient take rate (OPTR) is the number of successful PDX models generated/number of patients enrolled.

Harvest and passage procedures

Once the decision to harvest a xenograft was made, the mouse was brought to the laboratory and anesthesia was induced. The mouse was then sacrificed and tumor tissue was obtained by sharp dissection. A small piece of tumor was set aside and fixed in formalin for histologic confirmation. Any tissue from the first group of mice was considered first generation tissue, or F1 tissue. A second set of 5 NOD/SCID mice were implanted to form the second generation, or F2 generation (Fig. 1B), and any remaining tissue was cryopreserved utilizing similar methods to the original tumor as described above.

Histopathologic review

Tissue from all xenografts was reviewed by subspecialty trained hepatobiliary pathologists. Lymphoproliferation has been described to be a contamination problem in PDX series, and the

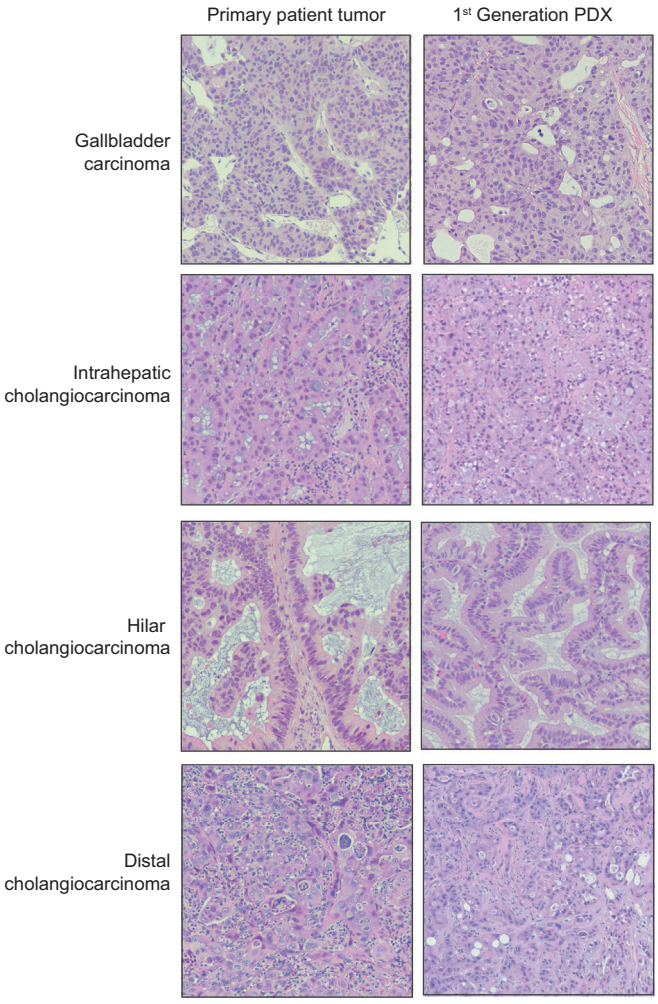

Fig. 2. Histological recapitulation seen in patient-derived xenografts. H&E staining of original patient tissue is recapitulated in the first generation of patient-derived xenografts in each of the four tumor subtypes: gallbladder carcinoma, intrahepatic cholangiocarcinoma, hilar cholangiocarcinoma, and distal cholangiocarcinoma. PDX, patient-derived xenograft.

purpose of pathologic review was to ensure that all xenografts were validated growths of biliary tract cancer and not lymphoproliferative tumors.[29,30]

Mate pair sequencing

Bulk resected tumor tissue was disrupted and the DNA was extracted using the Qiagen DNeasy Blood and Tissue kit (#69504) according to the manufacturer's instructions. The Mate Pair whole genome sequencing (MPseq) protocol was utilized to detect structural variants at gene level resolution through specialized larger 2–5 kb fragment tiling of the genome.[31–33] One microgram of DNA was applied to MPseq library preparation using the Nextera Mate-Pair Kit (Illumina, CA, FC-132-1001) following the manufacturer's instructions. Libraries were sequenced on the Illumina HiSeq4000 platform at a depth of 4 libraries per lane. Sequencing statistics data are presented in Fig. S1.

The binary indexing mapping algorithm developed by the Biomarker Discovery Lab at Mayo Clinic specifically for MPseq data, simultaneously maps both reads in a fragment to the GRCh38 reference genome.[34] Structural variants were detected using SVAtools, a suite of algorithms also developed by the Biomarker Discovery Lab at Mayo Clinic.[32] SVAtools specifically detects discordant fragments supporting a common junction (supporting-fragments) with powerful masks and filters to remove false-positive junctions. Copy number variant detection is performed using the read count of concordant fragments within non-overlapping bins.[33] Chromosomal copy levels and discordant mapping junctions are visualized on interactive software for genome plots.[31] Please see supplementary materials for more detailed MPseq methods.

Statistical analysis

Continous variables are presented as mean and SD unless they were not normally distributed, in which case they were presented as median and IQR. Categorical variables are presented as absolute and percentage of the total. For statistical analysis, Fisher's exact test and Pearson's chi squared were used for categorical variables and a 2-tailed Student's *t* test and ANOVA were used for continuous variables.

The Kaplan-Meier method was used for unadjusted survival analysis on patients who underwent curative-intent resections only. Overall survival was defined as the time in months from the date of surgery to the date of death and recurrence-free survival was defined as the time in months from the date of surgery to the date of recurrence. Patients alive or without recurrence at their last follow-up were censored. Cox proportional hazard regression was used to determine hazard ratios

Table 1. Xenograft growth metrics.

	All xenografts					
	Overall	**Gallbladder**	**iCCA**	**pCCA**	**dCCA**	***p* value**
OPTR (%)	47/87 (54.0)	7/10 (70.0)	23/41 (56.1)	8/20 (40.0)	9/16 (56.3)	0.43
	Successful xenografts					
	Overall	**Gallbladder**	**iCCA**	**pCCA**	**dCCA**	***p* value**
	n = 47	n = 7	n = 23	n = 8	n = 9	
TTF (days)	41 [26–84]	34 [25–97]	35 [23–82]	60 [22–103]	45 [40–107]	0.50
TTH (days)	130 [84–172]	169 [82–212]	115 [75–162]	168 [107–247]	131 [92–173]	0.36
Engraftment efficiency	0.6 [0.4–0.8]	0.5 [0.35–0.75]	0.6 [0.4–1]	0.6 [0.45–0.6]	0.7 [0.6–0.85]	0.50

OPTR: Number of successful PDX models/number of patients.
TTF: Number of days from implantation to palpation of first tumor (approximately 8 mm^3).
TTH: Number of days from implantation to harvest of first tumor (approximately 1,000 mm^3).
Engraftment efficiency: Number of mice with successful engraftment/number of total mice implanted.
CCA, cholangiocarcinoma; dCCA, distal cholangiocarcinoma; iCCA, intrahepatic cholangiocarcinoma; OPTR, overall patient take rate; PDX, patient-derived xenograft; TTF, time to tumor formation; TTH, time to tumor harvest.

(HRs) and 95% CIs. A p value of less than 0.05 was considered significant. All analyses were performed using JMP software (JMP Pro, Version 13.0.0, SAS Institute Inc, Cary, NC, USA).

Results

Patient and PDX characteristics

Between October 2013 and January 2018, 87 patients with histologically confirmed associated biliary tract malignancies were enrolled (Fig. S2). The most common tumor subtype implanted was intrahepatic cholangiocarcinoma (iCCA) with 41 (47.1%), followed by 20 perihilar cholangiocarcinomas (pCCA, 23.0%), 16 distal cholangiocarcinomas (dCCA, 18.4%), and 11 gallbladder cancers (GBCA, 11.5%). The median ischemic time for the specimens obtained from the operating room was longer than that of the specimens obtained from a radiographic biopsy (56 minutes *vs.* 30 minutes, p <0.01). Histologic recapitulation of original patient tumor morphology was observed consistently in all successfully validated xenografts (Fig. 2).

Of the 87 patients, 47 had successful PDX models for an OPTR of 54% (Table 1). Of these, 44 were obtained from surgery (94%) and only 3 were obtained by radiographic biopsy (7%) with a higher proportion of successful engraftment from surgical resection specimens compared to radiologic biopsy samples

Table 2. Patient and tumor characteristics.

	Unsuccessful engraftment (n = 40)	Successful engraftment (n = 47)	*p* value
	n (%)	n (%)	
Female	21 (52.5)	22 (46.8)	0.60
Median age at surgery [IQR]	64.4 [53.3–73.4]	54 [55.3–69]	0.58
Pathologic subtype			0.43
Gallbladder adenocarcinoma	3 (7.5)	7 (14.9)	
Intrahepatic cholangiocarcinoma	18 (45.0)	23 (48.9)	
Hilar cholangiocarcinoma	12 (30.0)	8 (17.0)	
Distal cholangiocarcinoma	7 (17.5)	9 (19.2)	
Neoadjuvant therapy			0.22
None	33 (82.5)	39 (83.0)	
Chemotherapy	5 (12.5)	7 (14.9)	
Radiation	0 (0.0)	1 (2.1)	
Chemotherapy and radiation	2 (5.0)	0 (0.0)	
Median initial CA19-9 [IQR]	90.5 [26–210]	53.5 [11.8–240.8]	0.41
Median pre-op CA19-9 [IQR]±	38.0 [19–132]	46.5 [24.0–97.3]	0.50
Procedure			0.36
Hepatectomy	18 (45.0)	24 (51.2)	
Biopsy (radiographic or in OR)	10 (25.0)	5 (10.6)	
Pancreatectomy	4 (10.0)	6 (12.8)	
Other	8 (20.0)	12 (25.6)	
Source of specimen			**0.03**
Operating room	31 (77.5)	44 (93.6)	
Radiographic biopsy	9 (22.5)	3 (6.4)	
Xenograft tissue obtained			0.09
Primary tumor	28 (70.0)	39 (83.0)	
Primary biopsy	9 (22.5)	3 (6.4)	
Metastatic lesion	3 (7.5)	5 (10.6)	
Median ischemic time [IQR]	41 [31–66]	61 [42–75]	**0.01**
Summary stage			0.23
0 – II	19 (48.7)	29 (61.7)	
III – IV	20 (51.3)	18 (38.3)	
Resected tumors only (Biopsies and metastatic lesions excluded)	**(n = 28)**	**(n = 39)**	***p* value**
Positive margins			0.06
Yes	6 (21.4)	2 (5.1)	
No	25 (78.6)	37 (94.9)	
Lymphovascular invasion			0.75
Yes	4 (14.3)	7 (18.0)	
No	24 (85.7)	32 (82.0)	
Perineural invasion			0.06
Yes	15 (53.6)	11 (28.2)	
No	13 (46.4)	28 (71.8)	
Tumor differentiation			0.95
Well	3 (10.7)	4 (10.3)	
Moderate/Poor	25 (89.3)	35 (89.7)	
Mean positive node ratio (SD)	0.12 (0.23)	0.14 (0.23)	0.79
Median tumor size [IQR]	4.5 [2.7–7.3]	3.9 [2.5–5.6]	0.41

Values in bold denote significance.
OR, operating room.
± Values for patients who underwent neoadjuvant therapy only (n = 14).

(59% *vs.* 25%, p = 0.03). No tumor growth (34/40, 85%) or development of lymphoproliferative tumors (6/40, 15%) accounted for the remaining failed tumor engraftments. Characteristics of successful engraftments compared to engraftment failures are listed in Table 2. Other than source of primary tumor samples (surgical specimen *vs.* radiologic biopsy), the only significant difference between the 2 groups was median ischemic time with the successfully engrafted xenografts having a longer ischemic time than the unsuccessful xenografts (61 minutes *vs.* 41 minutes, p = 0.01), however longer ischemic times were most often found in surgical specimens. There was no difference in pathologic tumor subtype, neoadjuvant status, initial or preoperative CA19-9, tumor differentiation, or clinical tumor stage.

Among the successfully engrafted tumors, the median TTF, TTH, and engraftment efficiency were 41 days, 130 days and 60%, respectively (Table 1). Of the 4 histologic subtypes, pCCAs had the longest median TTF at 60 days while GBCA had the longest median TTH at 169 days. There was no significant difference in TTF or TTH between the tumor subtypes.

Survival

Median follow-up for the entire patient cohort was 16 months [IQR 7–27] with 75 (86%) being obtained from curative-intent resections. Of these, 34 were iCCA (46%), 16 were pCCA (21%), 16 were dCCA (21%), and 9 were GBCA (12%). Median overall survival (OS) for the entire cohort was 35 months. On unadjusted Kaplan-Meier survival analysis, overall patient survival was not different between the engraftment failures and the successful engraftments (35 months *vs.* 32 months, p = 0.85) (Fig. 3A). However, recurrence-free survival was significantly different between the 2 groups, with engraftment failures having a median RFS that was not reached compared to only 12 months in patients with successful engraftments (p = 0.04) (Fig. 3B). This pattern remained on multivariable proportional hazard modeling with successful PDX engraftment being an independent predictor of worse RFS (HR 2.90; CI 1.27–6.60; p = 0.01) (Fig. 3C).

Genomic analysis

Of the 47 succesfully engrafted PDX models, 26 (55%) underwent further genomic characterization via MPseq analysis. Of these, all were obtained from curative-intent resections and 16 were iCCA (61%), 3 were pCCA (12%), 5 were dCCA (19%), and 2 were GBCA (8%). The genome profiles of 4 representative biliary tract PDX models are presented in Fig. S3, which reveal extensive aneuploid genomes, with gains and losses of distinct chromosomes. PDX #8 presents with a loss of entire copies of chromosomes 4, 6 and 21, with partial losses of 1p, 9p, and 18q (Fig. S3A). There are also gains of 1q and parts of 3q and 18p. DNA junctions reveal a complex chromoplectic rearrangement event with multiple junctions linking the centromeric region of chromosome 6 and 18q12. Chromothrypsis and chromplexy

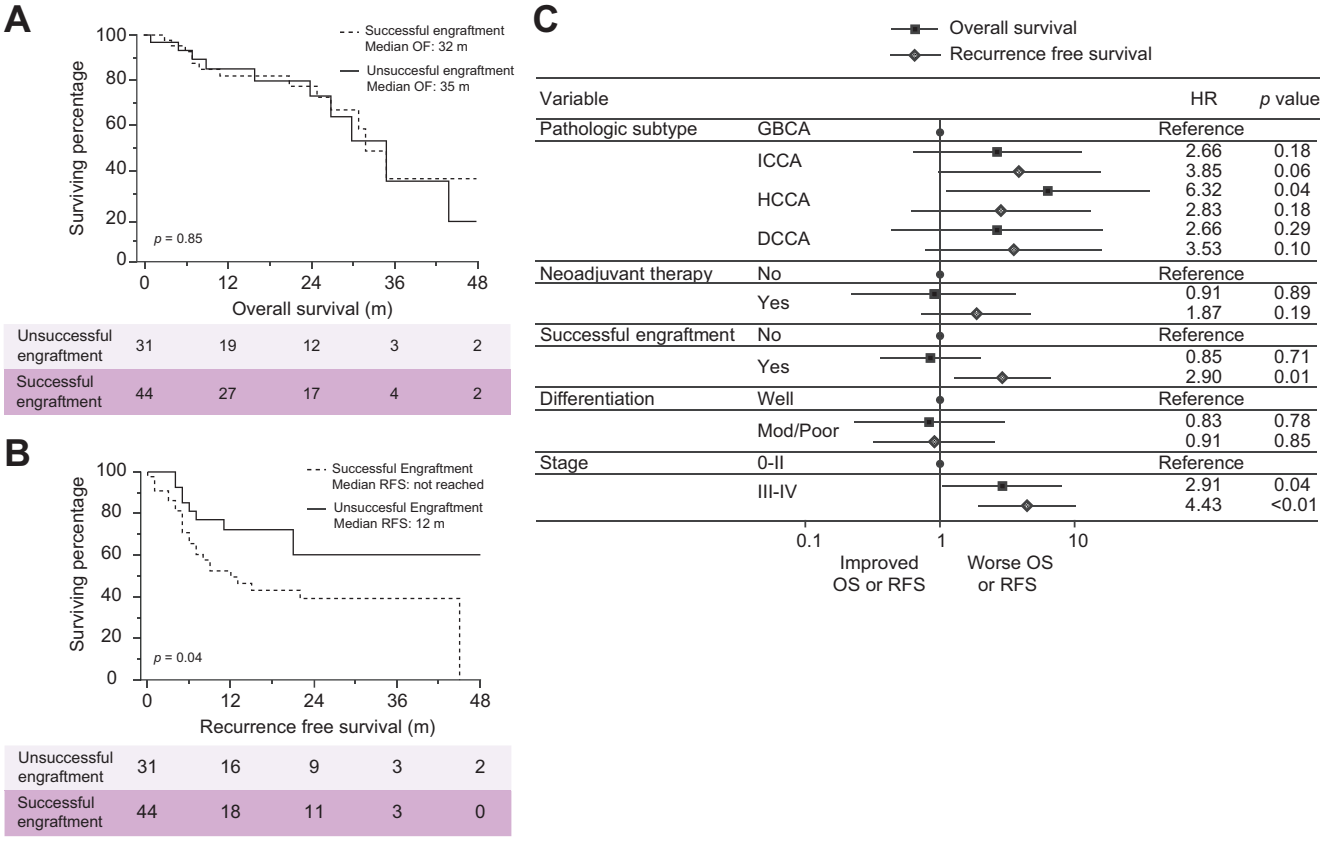

Fig. 3. Outcomes in patients with successful xenografts compared to patients with unsuccessful xenografts. Overall and recurrence free survival analysis of unsuccessful engraftsments compared to successful engraftments using unadjusted Kaplan-Meier analysis (A, B) and a multivariable Cox proportional hazard model (C). dCCA, distal cholangiocarcinoma; GBCA, gallbladder carcinoma; iCCA, intrahepatic cholangiocarcinoma; OS, overall survival; pCCA, perihilar cholangiocarcinoma; Mod, moderate; RFS, recurrence free survival.

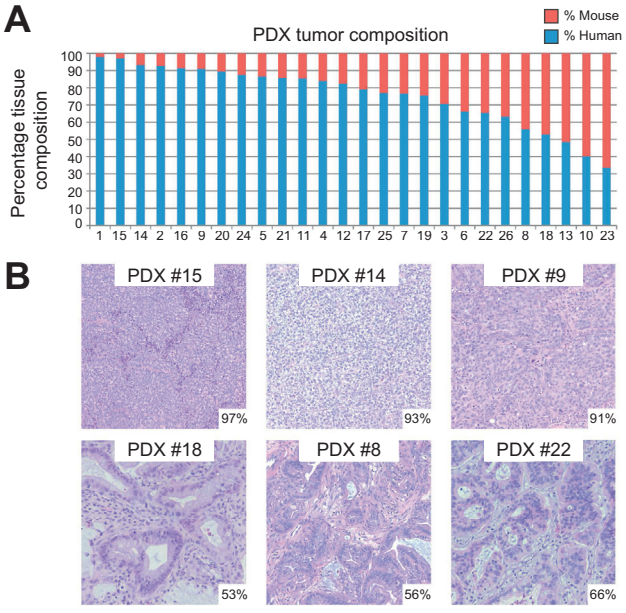

C

	≤82% human tissue n = 13	>82% human tissue n = 13	*p* value
Median TTF (days) [IQR]	77 [51-90]	75 [30-60]	0.01
Median TTH (days) [IQR]	126 [107-246]	75 [65-101]	<0.01

Fig. 4. Tumor composition and impact on PDX metrics. Predicted percentage of human and murine tissue in each biliary tract PDX tumor model (A) with representative examples indicating predicted percentage of human stroma in the lower right corner (B). Shorter TTF and TTH were associated with tumors containing a high percentage of human tissue (> median) with tumors containing a higher percentage of murine tissuer had slower growth metrics (C). PDX, patient-derived xenograft; TTF, time to tumor formation; TTH, time to harvest.

were common in the biliary tract tumors but often impacted distinct chromosomal regions. PDX #22 reveals an extensive chromoplectic event linking multiple chromosomes, including chromosomes 1, 3, 4, 10 and 13 (Fig. S3B). While PDX #17 contained a single chromplectic event linking the centromeric adjacent regions of 1q and 8p (Fig. S3C), PDX #16 predicts a tetraploid genome with extensive complex chromosomal shuffling involving over 50% of chromosomes (Fig. S3D).

Human stroma is rapidly replaced by murine stroma in PDX models within the first few generations of PDX propagation.[35] The fraction of the total number of fragments mapping to the human reference genome is indicative of the degree of murine stroma tissue in the tumors. Higher levels of murine stroma mapping reduce the actual tumor coverage from the total number of fragments mapped. Fig. 4A details the predicted percentage of human tumor present in each model, which ranged from 34% to 98%. Fig. 4B shows the histological correlation of the predicted percentage of human tumor compared to the level of stroma present in corresponding tumor tissue. Levels were adequate to detect junctions and copy level changes in all tumor models. The samples were dichotimized at the median percentage of human tumor present (81%) to assess the impact of composition. Tumors with higher human stroma composition grew at a faster rate compared to those with more murine stroma with shorter TTF (43 days *vs.* 77 days, p <0.01) and TTH (75 days *vs.* 126 days, p <0.01) (Fig. 4B). There were no other significant correlations with regard to survival, patient characteristics, or tumor features.

Loss of heterozygosity (LOH) was common in the biliary tract tumors. Fig. 5A presents the allelic copy level of key genes commonly altered in cholangiocarcinoma. *CDKN2A* was the most frequently deleted gene with 92% of cases losing 1 allele and 46% with biallelic loss. *CDKN2A* loss is an often reported early event in cholangiocarcinoma.[36] Fig. 5B illustrates examples of the different ways in which this is achieved in the tumor models. For PDX #8, PDX #22 and PDX #16, rearrangements in the *CDKN2A* locus result in homozygous loss of both copies of the gene (Fig. 5Bi-iii). In PDX #17, no loss of *CDKN2A* was observed (Fig. 5Biv) while PDX #10 has a single deletion event resulting in a homozygous loss of *CDKN2A* in a tetraploid background level of chromosome 9, indicating additional LOH for this chromosome (Fig. 5Bv). Overall survival was not significantly different in patients with single allele loss *vs.* patients with a biallelic loss (median OS 32 months *vs.* 21 months respectively, p = 0.24)

One gene allele copy was lost for *SMAD4, TP53, ARID1A* and *PTEN* in 77%, 58%, 54% and 31% of cases, with 1 case (PDX #22) predicting biallelic loss of PTEN. Allelic loss of *NRG1, FGFR1, FGFR2* and *FGFR3* genes were observed in 65%, 46%, 27% and 31% of cases. Functional driving fusions have also been reported in these genes and *NRG1* gene fusions were observed in 2 cases (PDX #12 and 17) and an amplification of *FGFR3* in PDX #20. Fig. 5C presents the commonly gained and lost chromosomal arms. The most commonly lost chromosomal arms are 9p, 18q, 8p and 17p, consistent with the commonly observed losses of *CDKN2A, SMAD4, NRG1* and *TP53*, respectively. Commonly gained genes were heavily influenced by the ploidy levels in the majority of cases, but 1q is gained in 20 of 26 cases (77%). Chromosome arm 2q is never observed lost in cholangiocarcinoma and 8q, 15q, 20q, 7p and 2p were each only observed lost in a single case, indicating potential essential functions in cholangiocarcinoma.

Tetraploid genomes were also commonly observed in the biliary tract tumors. Overall level of gains and losses of all chromosomal arms for the 26 biliary tract tumors are presented in Fig. 6. The 12 tumors in the top half of the figure predicted diploid genomes, while the lower 14 tumors containing extensive chromosomal gains with many predicted tetraploid genomes. Survival in patients with diploid *vs.* tetraploid genomes were significantly different. Patients with tetraploid genomes had significantly worse overall survival than those with diploid tumors (8 months *vs.* not reached, p <0.01) (Fig. 6B). Recurrence free survival was similarly worse in patients with tetraploid genomes (5 months *vs.* 9 months, p = 0.13) though this did not reach statistical significance (Fig. 6C). Additionally, tetraploid tumors were more likely to be higher stage (64% *vs.* 25%, p = 0.04) and were more likely to have lymphovascular invasion (57% *vs.* 17%, p = 0.03) (Fig. 6D).

Discussion

We have shown that biliary tract cancer PDX models can be successfully developed from various cancer subtypes with a high rate of engraftment, morphologic recapitulation of the original patient tumor, and genomic representation of biliary tract malignancies. Successful engraftment was an independent factor for an increased risk of recurrence in patients undergoing

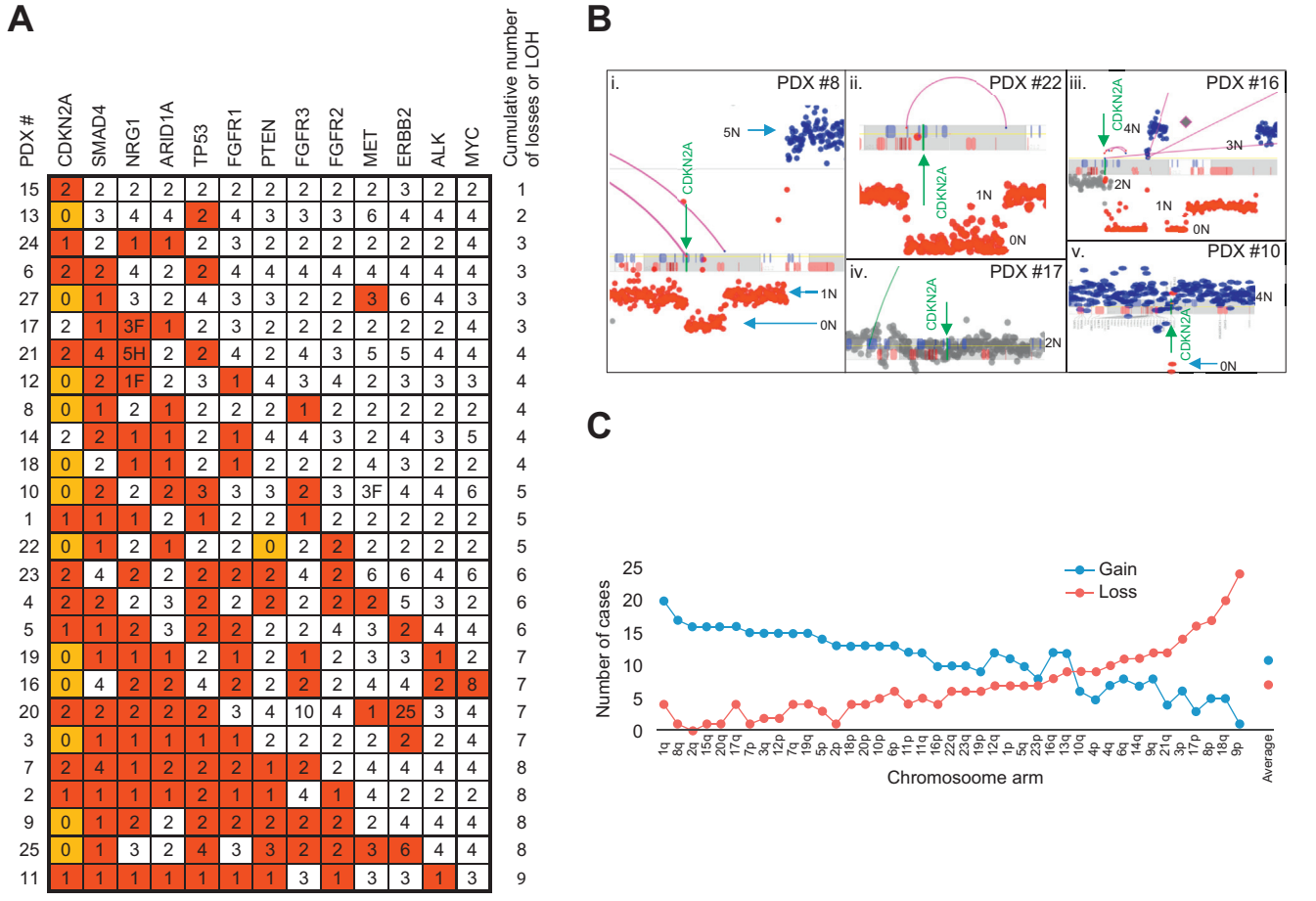

Fig. 5. Gene losses and loss of heterozygosity. Copy number changes of key genes. White, red, and orange shading indicates two alleles, loss of one allele, or loss of both alleles respectively. Numbers indicate the number of gene copies present in the genome. F and H indicate potential gene fusion and hit/potential truncation by a junction (A). Focal coverage of *CDKN2A* gene for (i) PDX #8, (ii) PDX #22, (iii), PDX #16, (iv) PDX #17, and (iv) PDX #10. 0N to 5N coverage levels indicated where appropriate with green arrow indicating location of *CDKN2A* gene (B). Number of cases with chromosomal arm gains or losses (loss or LOH) plotted (C). LOH, loss of heterozygosity; PDX, patient-derived xenograft.

curative intent resection. Additionally, biliary tract PDX tumors represent the genomic heterogeneity of human tumors with direct correlation to patient outcomes. This provides a greatly needed preclinical resource for pharmacological testing and treatment validation.

Previous studies involving PDX models have shown a correlation between clinical patient characteristics and successful PDX engraftment. Thomas and colleagues showed a significant decrease in recurrence-free survival in patients with pancreas ductal adenocarcinoma whose PDX successfully engrafted after previous neoadjuvant therapy.[22] Similar results have been described for a variety of tumor types, including colorectal cancer, breast cancer, and ovarian cancer.[37–39] Our study had similar findings with significant reductions in recurrence free survival for patients with successful PDX models. This positive correlation presents an opportunity to identify patients who are at a high risk for recurrence following their resection and also an opportunity to utilize the derived PDX tumors to identify potential therapies for clinical use prior to documented clinical recurrence.

The majority of the tissue specimens were obtained following surgical resection (86%) as opposed to radiographic biopsy (14%). The ischemic time for the surgical specimens was significantly longer than for that of radiographic biopsy (61 minutes *vs.* 41 minutes) which is likely due to the fact that after a specimen is surgically resected in our practice, it is initially evaluated in the frozen section pathology lab for a tissue diagnosis. Only after a tissue diagnosis has been made and surplus tissue has been verified is the tissue released for implantation. For radiographic biopsies, excess tissue cores are released immediately for implantation without being evaluated in the pathology lab and therefore the viability of such samples cannot be ascertained prior to implantation. Of the surgical specimens implanted, 44 of 75 (58.7%) were successful compared to only 3 of 12 (25%) obtained by radiographic biopsy and this was signficant predictor of successful engraftment. Therefore, despite longer ischemic time which has been shown to be a risk factor for failed PDX engraftment, a higher percentage of surgical xenografts successfully engrafted compared to the biopsy obtained specimens, likely due to acquisition of both larger and verified viable tumor specimens.

We have previously shown that biopsy tissue can be successfully used to generate PDX models in a number of different tumor types including cholangiocarcinoma, gallbladder,

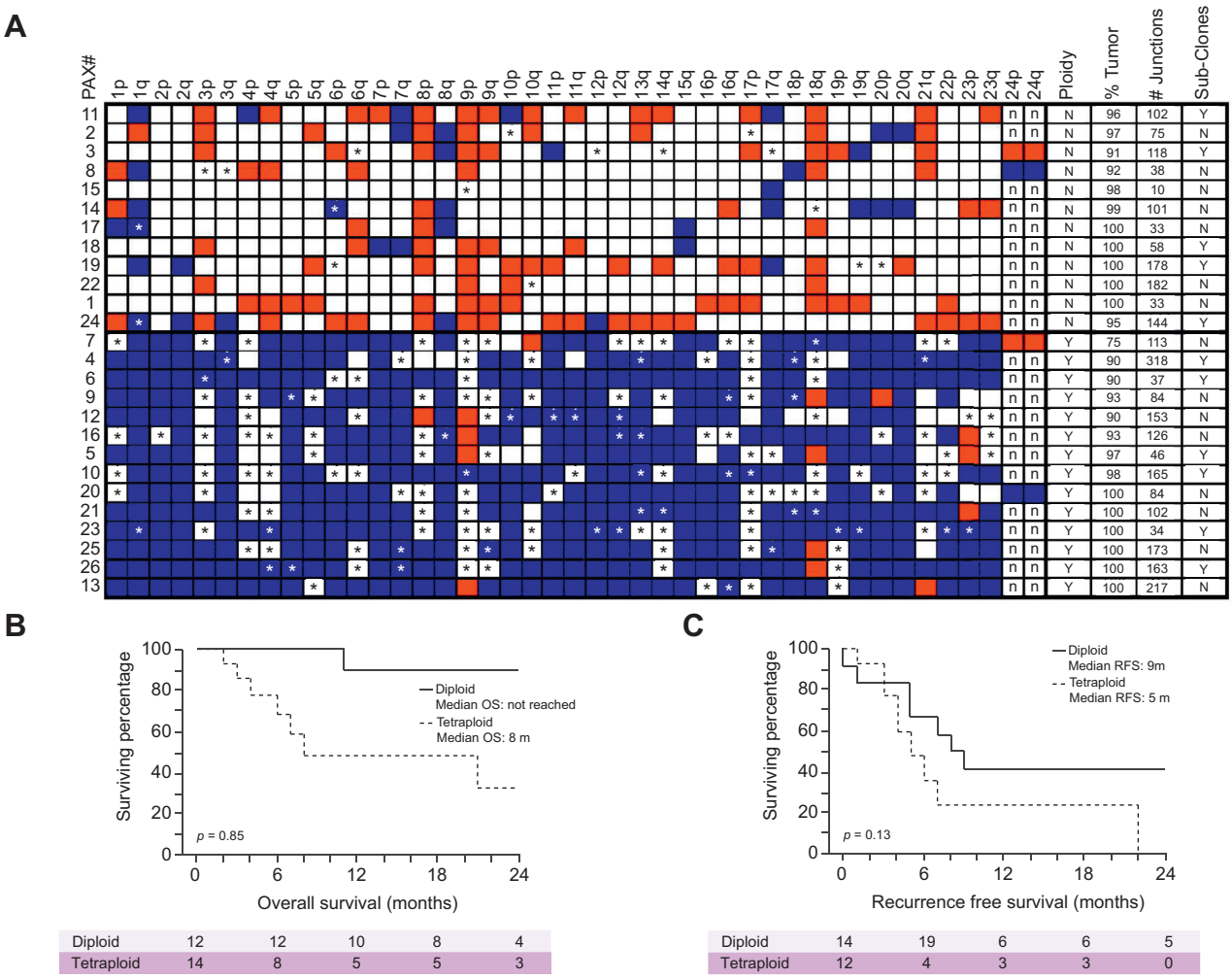

D

	Diploid n = 12	Tetraploid n = 14	*p* value
Stage III or IV (n (%))	3 (25.0)	9 (64.3)	0.04
Lymphovascular invasion (n (%))	2 (16.7)	8 (57.1)	0.03
Perineural invasion (n (%))	6 (50.0)	7 (50.0)	1.00
Moderate or poor differentiation (n (%))	11 (91.7)	12 (85.7)	0.64
Median TTF (days) [IQR]	55 [25-98]	47 [32-218]	0.74
Median TTH (days) [IQR]	120 [56-168]	124 [93-162]	0.66

Fig. 6. Chromosomal copy levels and clinical correlation. Chromosomal arm gains (blue) and losses (red). LOH indicated by *. Ploidy, percentage (%) tumor, number (#) of detected junctions and presence of sub-clonal populations indicated (A). Overall survival (B), recurrence free survival (C), and tumor characteristics (D) based on diploid or tetraploid genome status. LOH, loss of heterozygosity.

pancreas, and gastric cancer.[40] This is important as the majority of patients with biliary tract cancers are unable to be surgically resected at the time of their diagnosis, resulting in a large subset of patients whose tumors have not been xenografted. The disadvantage of biopsy-obtained specimens is that this usually required additional biopsy samples to be obtained which imposes a slightly increased risk for procedural complications, as well as for procuring non-viable or necrotic specimens that likely will not successfully engraft. This is not the case with surgically resected specimens in that surplus and confirmed viable tissue is obtained only after the surgical resection.

Our results show that MPseq can be used to efficiently process whole genome data from the murine PDX model and map the human sequences, allowing for accurate determination of murine stromal infiltration and revealing structural variants in biliary tract PDX models. The level of murine stromal infiltration varied greatly, from 34% to 98%, and correlated only to rate of growth in the PDX model with no correlation to patient characteristics, tumor characteristics, or passage number. A study examining the stromal composition in lung cancer PDX models showed a consistent stromal percentage over multiple passages of the tumor, suggesting that a paracrine interaction between

the human cancer cells and the stromal cells determines the specific tissue composition.[35] This high rate of variation is preserved in our biliary tract PDX models and may serve as a means to study the impact of stromal variability on treatment efficacy.

The PDX tumors were highly active for structural rearrangements and commonly had complex genomic rearrangements, though there was little similarity between tumors, again recapitulating the overall complexity of abnormalities seen in these challenging cancers despite their similar histologic phenotypes. Over 50% of the tumors predicted tetraploid genomes that strongly correlated with clinical outcomes. Patients who had tumors with diploid genomes had significantly longer survival compared to those who had tetraploid genomes. Of the 12 patients with diploid genomes, only 1 has died of disease and 5 have no evidence of disease greater than 2 years after resection. The prognostic value of tumor ploidy has previously been shown in primary patient tumors where diploidy was the best predictor for improved long-term survival.[41] The preservation of this genomic content again highlights the diverse applications of PDX models.

The PDX tumors profiled here showed a high rate of complete or single allele losses in genes previously shown to be altered in biliary tract tumors. *CDKN2A* was the most commonly altered gene with 46% of tumors having complete loss and an additional 46% with LOH. A previous analysis of 41 intrahepatic cholangiocarcinomas demonstrated 5% with a complete loss of *CDKN2A* and 20% with a LOH, though this was not found to be associated with survival.[42] Our analysis also found *CDKN2A* status to be unrelated to survival. Other highly altered genes were *SMAD4, NRG1, ARID1A,* and *TP53*, all of which have been found to be altered to varying degress in biliary tract tumors.[36,43] The absence of point mutation analysis for these models does not rule out the potential for additional pathogenic mutations in retained alleles of these genes, resulting in loss of function in the remaining allele equivalent to loss of both alleles. The patterns of chromosome gains and losses are also highly correlative to analyses of primary patient tumors.[44–46] Frequently lost chromosomes included 9p, 18q, 8p, and 17p which correspond to the genes with the most frequent losses: *CDKN2A, SMAD4, NRG1,* and *TP53*. These genomic alterations are representative of a cohort that are in desperate need of better therapies.

Limitations

There are several important limitations to the PDX model. The first is that there is a variable amount of human stromal displacement by murine stroma with multiple passages, with some studies reporting immediate replacement while others report a gradual replacement over time.[47,48] This change may influence the effectiveness of treatments that are affected by this interaction, though in our experience the replacement is always immediate. Another significant limitation to the PDX model is that the mice are not immunocompetent. The role of the immune system in cancer initiation and progression is becoming increasingly recognized and is unable to be investigated in this model.[49,50] What this model is able to offer is a reproduction of tumor heterogeneity that is seen in patients with similar histologic cancer types that is not available in other preclinical cancer models. The genomic analysis that we present is what has been found in our successful PDX models and was not compared to the original patient tumor. While there is certainly potential for mutational drift from the original tumor, our results are consistent with what is currently known about biliary tract tumors and we utilized only early generation PDX models for all genomic analyses to minimize this as a confounder. Lastly, the Kaplan-Meier survival analysis was performed with all tumor subtypes and is therefore quite heterogeneous, which may confound the overall results.

Conclusions

This is the largest series of biliary tract cancer xenografts reported to date. Despite longer ischemic time, succesful xenograft engraftment is superior for surgically resected specimens over radiographic tissue acquisition, suggesting that PDX engraftment should be attempted on surgical specimens if at all possible. Histologic and genomic analysis of patient-derived xenografts demonstrates accurate recapitulation of original tumor microstructures and genomic alterations. Development of biliary cancer xenografts is feasible. However, a surgeon-directed program is critical for technical success in order to minimize failure and maximize engraftment efficacy. Such programs provide a platform for substantial direct translational application for individualized medicine and data generated from the xenograft program are being used to direct adjuvant therapy.

Abbreviations

CCA, cholangiocarcinoma; dCCA, distal cholangiocarcinoma; ECM, extracellular matrix; GBCA, gallbladder carcinoma; HRs, hazard ratios; iCCA, intrahepatic cholangiocarcinoma; LOH, loss of heterozygosity; OPTR, overall patient take rate; OS, overall survival; pCCA, perihilar cholangiocarcinoma; PDX, patient-derived xenograft; TTF, time to tumor formation; TTH, time to tumor harvest.

Financial support

The authors acknowledge funding support from the Thrun Family and the Mayo Clinic Clinician Investigator Training program.

Conflicts of Interest

The authors declare no conflicts of interest that pertain to this work.

Please refer to the accompanying ICMJE disclosure forms for further details.

Authors' contributions

J.L., S.M., J.B., M.H., and M.T. conceived the concept and design. J.L., S.M., J.B., M.H., T.I., A.A., L.Y., I.L., and J.S. conducted the study and acquired the data. J.L., S.M., J.B., M.H., T.I., A.A., L.Y., I.L., J.S., S.C., D.N., M.T., R.G., L.R., G.G., R.S., and M.T. contributed to the analysis of the data the final manuscript.

Acknowledgement

The authors would like to thank the Biomarker Discovery Program of the Center for Individualized Medicine, specifically Dr. George Vasmatzis, for their support of this study.

Supplementary data

Supplementary data to this article can be found online at https://doi.org/10.1016/j.jhepr.2020.100068.

References

[1] Abdel-Rahman O, Elsayed Z, Elhalawani H. Gemcitabine-based chemotherapy for advanced biliary tract carcinomas. Cochrane Database Syst Rev 2018;4:CD011746.
[2] Rizvi S, Borad MJ, Patel T, Gores GJ. Cholangiocarcinoma: molecular pathways and therapeutic opportunities. Semin Liver Dis 2014;34:456–464.
[3] Wu K, Liao M, Liu B, Deng Z. ADAM-17 over-expression in gallbladder carcinoma correlates with poor prognosis of patients. Med Oncol 2011;28:475–480.
[4] Jarnagin WR, Gonon M, Fong Y, DeMatteo RP, Ben-Porat L, Little S, et al. Improvement in perioperative outcome after hepatic resection: analysis of 1, 803 consecutive cases over the past decade. Ann Surg 2002;236:397–407.
[5] Shubert CR, Habermann EB, Truty MJ, Thomsen KM, Kendrick ML, Nagorney DM. Defining perioperative risk after hepatectomy based on diagnosis and extent of resection. J Gastrointest Surg 2014;18:1917–1928.
[6] Groot Koerkamp B, Fong Y. Outcomes in biliary malignancy. J Surg Oncol 2014;110:585–591.
[7] DeOliveira ML, Cunningham SC, Cameron JL, Kamangar F, Winter JM, Lillemoe KD, et al. Cholangiocarcinoma: thirty-one-year experience with 564 patients at a single institution. Ann Surg 2007;245:755–762.
[8] Razumilava N, Gores GJ. Cholangiocarcinoma. Lancet 2014;383:2168–2179.
[9] Valle J, Wasan H, Palmer DH, Cunningham D, Anthoney A, Maraveyas A, et al. Cisplatin plus gemcitabine versus gemcitabine for biliary tract cancer. N Engl J Med 2010;362:1273–1281.
[10] Misra S, Chaturvedi A, Misra NC, Sharma ID. Carcinoma of the gallbladder. Lancet Oncol 2003;4:167–176.
[11] Maria Cekanova KR. Animal models and therapeutic molecular targets of cancer: utility and limitations. Drug Des Devel Ther 2014;2014:1911–1922.
[12] Siolas D, Hannon GJ. Patient-derived tumor xenografts: transforming clinical samples into mouse models. Cancer Res 2013;73:5315–5319.
[13] Wenger SL, Senft JR, Sargent LM, Bamezai R, Bairwa N, Grant SG. Comparison of established cell lines at different passages by karyotype and comparative genomic hybridization. Biosci Rep 2004;24:631–639.
[14] Hausser H-J, Brenner RE. Phenotypic instability of Saos-2 cells in long-term culture. Biochem Biophys Res Commun 2005;333:216–222.
[15] Edeleva EV, Shcherbata HR. Stress-induced ECM alteration modulates cellular microRNAs that feedback to readjust the extracellular environment and cell behavior. Front Genet 2013;4:305.
[16] Pickup MW, Mouw JK, Weaver VM. The extracellular matrix modulates the hallmarks of cancer. EMBO Rep 2014;15:1243–1253.
[17] Hamdan FH, Zihlif MA. Gene expression alterations in chronic hypoxic MCF7 breast cancer cell line. Genomics 2014;104:477–481.
[18] Michor F, Weaver VM. Understanding tissue context influences on intratumour heterogeneity. Nat Cell Biol 2014;16:301–302.
[19] Gillet J, Maria A, Varma S, Marino M, Green LJ, Vora MI, et al. Redefining the relevance of established cancer cell lines to the study of mechanisms of clinical anti-cancer drug resistance. Proc Natl Acad Sci USA 2011;108:18708–18713.
[20] Hidalgo M, Amant F, Biankin AV, Budinská E, Byrne AT, Caldas C, et al. Patient-derived xenograft models: an emerging platform for translational cancer research. Cancer Discov 2014;4:998–1013.
[21] Tentler JJ, Tan AC, Weekes CD, Jimeno A, Leong S, Pitts TM, et al. Patient-derived tumour xenografts as models for oncology drug development. Nat Rev Clin Oncol 2012;9:338–350.
[22] Thomas RM, Truty MJ, Kim M, Kang Y, Zhang R, Chatterjee D, et al. The canary in the coal mine: the growth of patient-derived tumorgrafts in mice predicts clinical recurrence after surgical resection of pancreatic ductal adenocarcinoma. Ann Surg Oncol 2015;22:1884–1892.
[23] Wang C, Lv H, Yang W, Li T, Fang T, Lv G, et al. SVCT-2 determines the sensitivity to ascorbate-induced cell death in cholangiocarcinoma cell lines and patient derived xenografts. Cancer Lett 2017;398:1–11.
[24] Wang Y, Ding X, Wang S, Moser CD, Shaleh HM, Mohamed EA, et al. Antitumor effect of FGFR inhibitors on a novel cholangiocarcinoma patient derived xenograft mouse model endogenously expressing an FGFR2-CCDC6 fusion protein. Cancer Lett 2016;380:163–173.
[25] Cavalloni G, Peraldo-Neia C, Sassi F, Chiorino G, Sarotto I, Aglietta M, et al. Establishment of a patient-derived intrahepatic cholangiocarcinoma xenograft model with KRAS mutation. BMC Cancer 2016;16:90.
[26] Zhan M, Yang RM, Wang H, He M, Chen W, Xu SW, et al. Guided chemotherapy based on patient-derived mini-xenograft models improves survival of gallbladder carcinoma patients. Cancer Commun 2018;38:1–9.
[27] Ojima H, Yamagishi S, Shimada K, Shibata T. Establishment of various biliary tract carcinoma cell lines and xenograft models for appropriate preclinical studies. World J Gastroenterol 2016;22:9035–9038.
[28] Obeid JS, McGraw CA, Minor BL, Conde JG, Pawluk R, Lin M, et al. Procurement of shared data instruments for Research Electronic Data Capture (REDCap). J Biomed Inform 2013;46:259–265.
[29] Leiting JL, Hernandez MC, Yang L, Bergquist JR, Ivanics T, Graham RP, et al. Lymphoproliferative tumor formation in hepatopancreaticobiliary and gastrointestinal cancer patient-derived xenografts. Sci Rep 2019;9:5901.
[30] Bondarenko G, Ugolkov A, Rohan S, Kulesza P, Dubrovskyi O, Gursel D, et al. Patient-derived tumor xenografts are susceptible to formation of human lymphocytic tumors. Neoplasia 2015;17:735–741.
[31] Gaitatzes A, Johnson SH, Smadbeck JB, Vasmatzis G. Genome U-Plot: a whole genome visualization. Bioinformatics 2018;34:1629–1634.
[32] Johnson SH, Smadbeck JB, Smoley SA, Gaitatzes A, Murphy SJ, Harris FR, et al. SVAtools for junction detection of genome-wide chromosomal rearrangements by mate-pair sequencing (MPseq). Cancer Genet 2018;221:1–18.
[33] Smadbeck JB, Johnson SH, Smoley SA, Gaitatzes A, Drucker TM, Zenka RM, et al. Copy number variant analysis using genome-wide mate-pair sequencing. Genes Chromosomes Cancer 2018;57:459–470.
[34] Drucker TM, Johnson SH, Murphy SJ, Cradic KW, Therneau TM, Vasmatzis G. BIMA V3: an aligner customized for mate pair library sequencing. Bioinformatics 2014;30:1627–1629.
[35] Rudin CM, Schneeberger VE, Allaj V, Gardner EE, Poirier JT. Quantitation of murine stroma and selective purification of the human tumor component of patient-derived xenografts for genomic analysis. PLoS One 2016;11(9):e0160587.
[36] Churi CR, Shroff R, Wang Y, Rashid A, Kang HSC, Weatherly J, et al. Mutation profiling in cholangiocarcinoma: prognostic and therapeutic implications. PLoS One 2014;9:1–23.
[37] Eoh KJ, Chung YS, Lee SH, Park SA, Kim HJ, Yang W, et al. Comparison of clinical features and outcomes in epithelial ovarian cancer according to tumorigenicity in patient-derived xenograft models. Cancer Res Trea 2018;50:956–963.
[38] McAuliffe PF, Evans KW, Akcakanat A, Chen K, Zheng X, Zhao H, et al. Ability to generate patient-derived Breast cancer xenografts is enhanced in chemoresistant disease and predicts poor patient outcomes. PLoS One 2015;10:1–20.
[39] Oh BY, Lee WY, Jung S, Hong HK, Nam D-H, Park YA, et al. Correlation between tumor engraftment in patient-derived xenograft models and clinical outcomes in colorectal cancer patients. Oncotarget 2015;6:16059–16068.
[40] Hernandez MC, Bergquist JR, Leiting JL, Ivanics T, Yang L, Smoot RL, et al. Patient-derived xenografts can be reliably generated from patient clinical biopsy specimens. J Gastrointest Surg 2019;23(4):818–824.
[41] Abou-Rebyeh H, Al-Abadi H, Jonas S, Rotter I, Bechstein WO, Neuhaus P. DNA analysis of cholangiocarcinoma cells: prognostic and clinical importance. Cancer Detect Prev 2002;26:313–319.
[42] Tannapfel A, Benicke M, Katalinic A, Uhlmann D, Köckerling F, Hauss J, et al. Frequency of p16(INK4A) alterations and K-ras mutations in intrahepatic cholangiocarcinoma of the liver. Gut 2000;47:721–727.
[43] Cristescu R, Lee J, Nebozhyn M, Kim KM, Ting JC, Wong SS, et al. Molecular analysis of gastric cancer identifies subtypes associated with distinct clinical outcomes. Nat Med 2015;21:449–456.
[44] Dalmasso C, Carpentier W, Guettier C, Camilleri-Broët S, Borelli WV, Campos dos Santos CR, et al. Patterns of chromosomal copy-number alterations in intrahepatic cholangiocarcinoma. BMC Cancer 2015;15:1–11.
[45] Sakurai-Yageta M, Pairojkul C, Yongvanit P, Murakami Y, Goto A, Ito T. Genomic and transcriptional alterations of cholangiocarcinoma. J Hepatobiliary Pancreat Sci 2014;21:380–387.
[46] Rijken AM, Hu J, Perlman EJ, Morsberger LA, Long P, Kern SE, et al. Genomic alterations in distal bile duct carcinoma by comparative genomic hybridization and karyotype analysis. Genes Chromosom Cancer 1999;26:185–191.
[47] Bergamaschi A, Hjortland GO, Triulzi T, Sørlie T, Johnsen H, Ree AH, et al. Molecular profiling and characterization of luminal-like and basal-like in vivo breast cancer xenograft models. Mol Oncol 2009;3:469–482.
[48] Mattie M, Christensen A, Chang MS, Yeh W, Said S, Shostak Y, et al. Molecular characterization of patient-derived human pancreatic tumor xenograft models for preclinical and translational development of cancer therapeutics. Neoplasia 2013;15:1138–1150.
[49] Mendes F, Domingues C, Rodrigues-Santos P, Abrantes AM, Gonçalves AC, Estrela J, et al. The role of immune system exhaustion on cancer cell escape and anti-tumor immune induction after irradiation. Biochim Biophys Acta - Rev Cancer 2016;1865:168–175.
[50] Janssen LME, Ramsay EE, Logsdon CD, Overwijk WW. The immune system in cancer metastasis: friend or foe? J Immunother Cancer 2017;5:1–14.